Optics Letters

Quasiperiodic one-dimensional photonic crystals with adjustable multiple photonic bandgaps

Andrey M. Vyunishev,[1,2,*] Pavel S. Pankin,[2,3] Sergey E. Svyakhovskiy,[4] Ivan V. Timofeev,[1,3] and Stepan Ya. Vetrov[1,2]

[1]Kirensky Institute of Physics, Federal Research Center KSC SB RAS, Krasnoyarsk 660036, Russia
[2]Institute of Engineering Physics and Radio Electronics, Siberian Federal University, Krasnoyarsk 660041, Russia
[3]Institute of Nanotechnology, Spectroscopy and Quantum Chemistry, Siberian Federal University, Krasnoyarsk 660041, Russia
[4]Department of Physics, M.V. Lomonosov Moscow State University, Moscow 119991, Russia
*Corresponding author: vyunishev@iph.krasn.ru

Received 28 July 2017; revised 17 August 2017; accepted 17 August 2017; posted 21 August 2017 (Doc. ID 303483); published 12 September 2017

We propose an elegant approach to produce photonic bandgap (PBG) structures with multiple photonic bandgaps by constructing quasiperiodic photonic crystals (QPPCs) composed of a superposition of photonic lattices with different periods. Generally, QPPC structures exhibit both aperiodicity and multiple PBGs due to their long-range order. They are described by a simple analytical expression, instead of quasiperiodic tiling approaches based on substitution rules. Here we describe the optical properties of QPPCs exhibiting two PBGs that can be tuned independently. PBG interband spacing and its depth can be varied by choosing appropriate reciprocal lattice vectors and their amplitudes. These effects are confirmed by the proof-of-concept measurements made for the porous silicon-based QPPC of the appropriate design.

OCIS codes: (230.5298) Photonic crystals; (290.4210) Multiple scattering; (350.2460) Filters, interference.

https://doi.org/10.1364/OL.42.003602

Photonic crystals (PCs) have attracted much attention in the last decades since the concept was introduced [1]. The main feature of PCs is the existence of the photonic bandgap (PBG) with prohibited transmission [1,2]. The insertion of a defect layer into PCs breaks the periodicity and results in the appearance of a defect mode placed within the PBG, which can be used for spectral filtering. Depending on their composition, PCs can conditionally be distinguished as periodic, quasiperiodic photonic crystals (QPPCs) and aperiodic PCs. There are common ways for the formation of QPPCs, which are also called deterministic aperiodic structures [3] or tilings, and are the intermediate between the periodic and aperiodic PCs. Some substitution rule representing a mathematical sequence in layer positions has to be introduced to interleave layers with different refractive indices to form a QPPC structure. So far, several kinds of QPPCs have been investigated; among them are Fibonacci, Thue–Morse, Rudin–Shapiro, double-periodic, Octonacci, Cantor, and Pell structures [4]. Earlier, deterministic PCs were successfully used for optical filtering, multi-frequency terahertz manipulation, near-perfect absorption and omnidirectional reflection, and photoluminescence emission enhancement [5–12]. Fibonacci and Thue–Morse-like photonic structures have been reported for the Bloch-like surface waves [13] and multimode photon-exciton coupling [14], which represent a significant advantage compared to periodic PC counterparts. Alternatively, the introduction of random deviations into layer thicknesses or refractive indices violates the periodicity of a structure, thus leading to the widening of PBGs [15–17]. Another kind of 1D PC structures represents a logical combination of two one-dimensional (1D) PCs of close periods [18]. The transmission spectrum of these structures demonstrates the frequency region with a finite number of slow modes. Recently, Alagappan and Png considered a dual-periodic structure obtained by the summation of the two harmonic functions [19]. Such structures can be used for designing high-quality, broadband, and multichannel slow light devices to create a new class of passive superluminal structures. Nevertheless, the formation of deterministic PC structures with required optical characteristics is complicated, and secondary (parasitic) PBGs may appear.

In this Letter, we propose a way for the composition of QPPCs with pre-designed multiple PBGs. The QPPC is constructed by a superposition of several spatial harmonics with different spatial frequencies that determine the spectral position of multiple PBGs. We show that the spectra of such QPPCs represent a combination of those for the two conjugated periodic 1D PCs. To the best of our knowledge, such an approach has not been applied for the composition of linear PCs, while it has been considered in nonlinear optics for the multi-wavelength conversion [20,21] and multiple spatial harmonic generation [22].

The refractive index of the proposed linear QPPC structure is described by

$$n(z) = n_0 + \Delta n \operatorname{sgn}\left(\sum a_j \sin[\mathbf{G}_j z + \phi_j]\right). \quad (1)$$

Here n_0 is the average refractive index; Δn is the maximum deviation of the refractive index from its average value n_0; a_j, $\mathbf{G}_j$

and ϕ_j are the amplitude, reciprocal lattice vector (RLV), and relative phase of the jth spatial harmonic; $\mathrm{sgn}(x) = |x|/x$ is a signum function. We restrict our consideration by the case of two RLVs, so that Eq. (1) is simplified to

$$n(z) = n_0 + \Delta n\,\mathrm{sgn}(a_1 \sin \mathbf{G}_1 z + a_2 \sin \mathbf{G}_2 z). \quad \textbf{(2)}$$

We study the spatial and spectral characteristics of the QPPC in comparison to the 1D PC with $\mathbf{G}_1$ and $\mathbf{G}_2$. In the plane wave approximation, and for the linearly polarized waves, the wave propagation in arbitrary structured PC and respective transmission coefficients can be calculated using the transfer-matrix formalism [23]. The modulation of the refractive index becomes a periodic one if any of two amplitudes in Eq. (2) equals zero ($a_2 = 0$). The period of the structure is $\Lambda = 2\pi/|\mathbf{G_1}|$, and its Fourier transformation demonstrates a maximum at the spatial frequency G_1 [Fig. 1(b)]. As a result, the first-order PBG in the transmission spectrum appears and corresponds to the RLV G_1 [Fig. 2(a)], which has a spectral position that satisfies the Bragg condition [1,2]:

$$\lambda_m = 2\pi(n_1 + n_2)/mG_1, \quad \textbf{(3)}$$

where $n_{1,2}$ are the refractive indices of the PC constituting layers.

Keeping both terms in Eq. (2), we get a more complicated spatial modulation of the refractive index corresponding to the QPPC structure [Fig. 1(a)]. In our calculation, we used the parameters that were taken for the fabrication of the porous silicon QPPC described below. So we took $n_0 = 1.40$, $\Delta n = 0.08$, $a_1 = a_2$, $|\mathbf{G}_1| = 26.7$ rad $\cdot$ μm^{-1}, and $|\mathbf{G}_2| = 35.6$ rad $\cdot$ μm^{-1}. The period of the QPPC structure is $\Lambda = 2\pi/|\mathbf{G_3}|$, where $|\mathbf{G}_3| = G_3$ is the highest common factor of $\{G_1, G_2\}$. If G_2/G_1 is a rational number, then Λ is a finite number and the structure possesses the translational symmetry. In the case under study, the highest common factor G_3 is 8.9 rad $\cdot$ μm^{-1}. Then the period of the QPPC equals 0.706 μm, and 12 periods fall on the thickness of the QPPC. The QPPC period contains eight layers in a unit cell. Such a structure differs from common 1D PCs based on bilayer structures, or even of a more specific case of three-layered structures described previously (see, e.g., [24,25]). In our case, the proper choice of RLVs can provide the unit cell consisting of an arbitrary number of layers; therefore, the unit cell may exceed an overall thickness of the structure. The Fourier spectrum of the structure described by Eq. (2) demonstrates the presence of two peaks corresponding to the spatial frequencies G_1 and G_2, instead of one at G_3 arising from the periodicity of the QPPC structure [Fig. 1(b)]. Accounting for an interplay between the spatial and spectral characteristics, we expect the appearance of the two PBGs with the spectral positions defined by Eq. (3). Indeed, the calculated transmission spectrum of the QPPC confirms this assumption [Fig. 2(b)]: one can see the presence of two PBGs with the central wavelength corresponding to that of periodic PCs, as is shown in Fig. 2(a). In general, the PBG central wavelengths can be found from Eq. (3) by substituting the values G_1 and G_2. In this case, the ratio of G_1 to G_2 is 3∶4 and, the PBG central wavelengths are given by G_3 with multipliers $m = 3$ and 4, respectively. Our calculations demonstrate that optical waves undergo the selective Bragg diffraction for both RLVs. Note that the approach provides the Fourier amplitudes for relevant RLVs as high as possible, which is evident from the comparison of the QPPC and the two conjugated PCs shown in Fig. 1(b). This makes QPPCs differing from other deterministic PCs (see, e.g., [5–12]), where a series of parasitic PBGs is exhibited.

Compare the QPPC with more straightforward implementation of a PC stacked by two conjugated periodic PCs with the primary spatial frequencies $G_{1,2}$. Figure 2(b) shows calculated transmission spectra for the QPPC and for the conjugated PC stacked by two 4.5-μm thick periodic PCs. For the conjugated PCs, the edges and the bottom of the PBGs suffer from distortions, while a QPPC provides PBGs with smooth and sharp edges. Moreover, the average interband transmittance of the QPPC manifests weaker oscillations. The same difference is deduced from the analysis of the Fourier spectra of both structures [Fig. 1(b)].

For the proof-of-concept experiments, the QPPC based on mesoporous silicon is fabricated by electrochemical etching of crystalline silicon [26]. The refractive indices of the layers were 1.32 and 1.48, providing $n_0 = 1.40$ and $\Delta n = 0.08$.

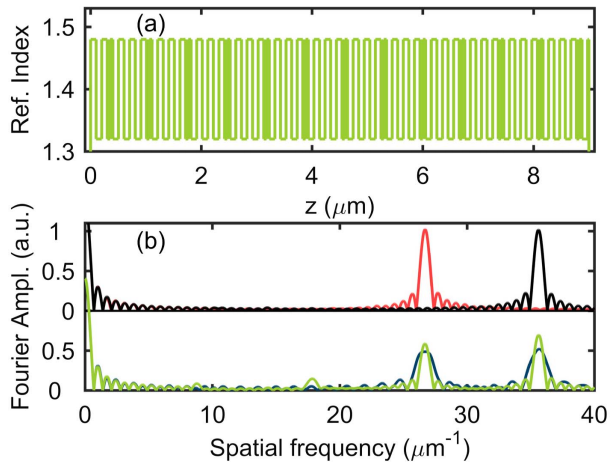

Fig. 1. (a) Modulation of the refractive index calculated using Eq. (2); (b) the Fourier transform of the refractive index as a function of the spatial coordinate for the periodic PC (red and black), conjugated PC (indigo), and the QPPC (yellow-green) structures.

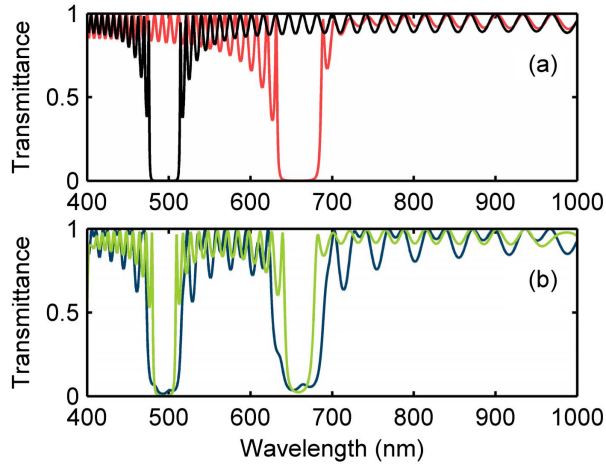

Fig. 2. (a) Calculated transmission spectral dependencies for a periodic PC with $|\mathbf{G}_1| = 26.7$ rad $\cdot$ μm^{-1} (red) and $|\mathbf{G}_2| = 35.6$ rad $\cdot$ μm^{-1} (black). (b) Calculated transmission spectra for the conjugated PCs (indigo) and the QPPC (yellow-green).

Table 1. Predesigned and Fitted Values of RLV G_2 and Measured and Calculated [Eq. (3)] PBG Central Wavelengths at Fixed $G_1 = 26.7$ rad · μm^{-1}

Sample #	Predesigned G_2 rad · μm^{-1}	Fitted G_2 rad · μm^{-1}	$\lambda_{meas.}$ (nm)	$\lambda_{calc.}$ (nm)
1	17.8	18.1	976	972
2	22.2	22.4	790	785
3	26.7	26.8	655	657
4	31.1	30.9	570	570
5	35.6	37.9	464	464
6	40.0	44.3	398	397

The structure has the thickness 9 μm and contains 52 layers. As shown in Fig. 3, the measured QPPC transmission spectra demonstrate two PBGs centered at 494 and 660 nm, respectively. The refractive indices and primary RLV were reasonably tuned to obtain a good agreement between calculated and measured transmission spectra. The designed and fitted values of G_2 are given in Table 1. The adjustment of these values is imposed by the uncertainty inherent to the sophisticated fabrication method of the QPPC. Nevertheless, it can be deduced that the proper choice of RLVs can fit the transmittance dependencies of the QPPC. In addition, by varying the amplitudes a_j in Eq. (1), we can distribute the ratio of transmittance or reflectance between the individual PBGs.

In order to reveal the dependence of the transmission spectra on the continuous variation of the ratio of G_1 and G_2, we made a set of structures with the fixed G_1 and varied G_2 values. The PBG corresponding to G_2 shifts towards short wavelengths while increasing the value of G_2 (Fig. 4). The PBG for G_1 keeps its position except for a small spectral shift in the vicinity of the PBG crossing point at $|G_2| = |G_1|$, corresponding to the single periodic PC. The adjustment of the spatial frequencies G_1 and G_2 is used to form the passband with an arbitrary width in the visible spectral range. Moreover, a set of additional narrow PBGs appears inside the passbands. It can be seen that these PBGs are equidistant in the frequency domain and correspond to the Fourier transform peaks of Fig. 1(b) with the spatial frequency increment G_3. They originate from a nonharmonic spatial profile of the dielectric permittivity and are well evaluated using the coupled mode theory (see Ch. 12 of [27]). These PBGs represent the mirror counterpart of the primary PBGs in the frequency domain.

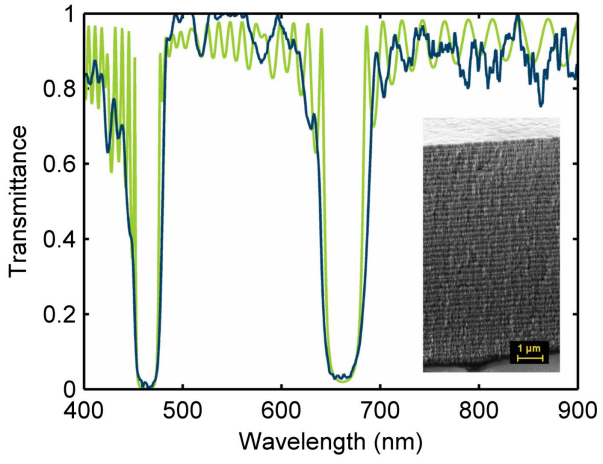

Fig. 3. Measured (indigo) and calculated (yellow-green) transmission spectral dependence of the QPPC with $G_1 = 26.7$ rad · μm^{-1} and $G_2 = 35.6$ rad · μm^{-1}. Inset: SEM image of the porous silicon-based QPPC structure (Sample 5 from Table 1).

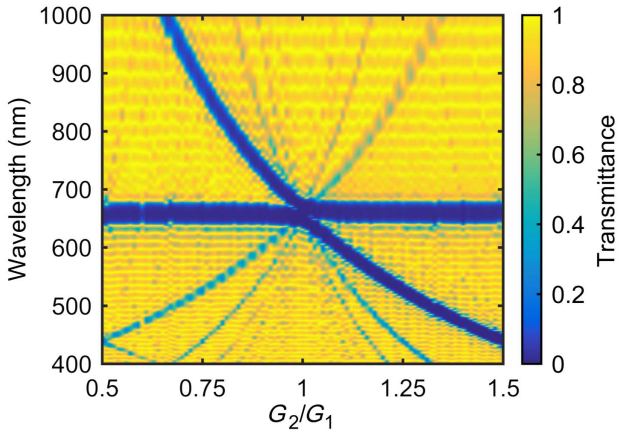

Fig. 4. Calculated transmission spectral dependence of the QPPC versus the fraction G_2/G_1.

Figure 5 shows the measured transmittance spectra for all QPPC samples *versus* the value of G_2. It is clearly seen that the PBG corresponding to G_2 exhibits a pronounced spectral shift. The experimental results are in a good agreement with the numerical results shown in Fig. 4. The experimental and theoretical results are summarized in Table 1. As one can see, the fitted values G_2 are close enough to the predesigned values, and the PBG central wavelengths calculated for fitted RLV G_2 are in the vicinity of the measured values.

The analysis of the transmission and reflectance spectra allowed us to estimate the attenuation of the sample by 1.2 cm^{-1} at 670 nm. This value is higher than the absorption of amorphous quartz. This discrepancy can be explained by the light scattering on the layer interfaces.

Summing up, we propose a versatile approach of refractive index superposition modulation for structuring QPPCs with

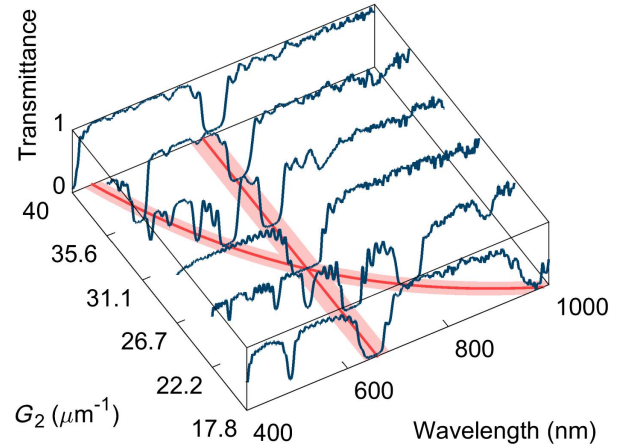

Fig. 5. Measured transmission spectra of the QPPC (indigo) on the value G_2 and corresponding PBG central wavelength positions calculated by using Eq. (3) (red).

adjustable multiple bandgaps. The obtained results show that the light undergoes the selective Bragg diffraction resulting from a long-range order of the QPPC. PBGs' spectral positions and their depths can be specified prior to the fabrication by the proper choice of RLVs. The approach proposed can be extended to a wide range of wave phenomena of arbitrary nature in periodic structures in areas such as acousto-optics, plasmonics, and magnonics.

Funding. Government of Krasnoyarsk Territory, Krasnoyarsk Region Science and Technology Support Fund (16-42-243065); Russian Foundation for Basic Research (RFBR) (16-02-01100); Scholarship of the President of the Russian Federation (SP-3372.2015.5, SP-227.2016.5).

Acknowledgment. The authors thank Prof. T. V. Murzina, M. Y. Shalaginov, and Prof. V. M. Shalaev for help and fruitful discussions.

REFERENCES

1. E. Yablonovitch, Phys. Rev. Lett. **58**, 2059 (1987).
2. J. D. Joannopoulos, S. G. Johnson, J. N. Winn, and R. D. Meade, *Photonic Crystals: Molding the Flow of Light* (Princeton University, 2011).
3. L. Dal Negro, *Optics of Aperiodic Structures: Fundamentals and Device Applications* (CRC Press, 2013).
4. Z. V. Vardeny, A. Nahata, and A. Agrawal, Nat. Photonics **7**, 177 (2013).
5. M. S. Vasconcelos, P. W. Mauriz, and E. L. Albuquerque, Microelectron. J. **40**, 851 (2009).
6. Y. Qin, C. Zhang, D. Zhu, Y. Zhu, H. Guo, G. You, and S. Tang, Opt. Express **17**, 11558 (2009).
7. Y. Gong, X. Liu, L. Wang, H. Lu, and G. Wang, Opt. Express **19**, 9759 (2011).
8. H.-F. Zhang, J.-P. Zhen, and W.-P. He, Optik **124**, 4182 (2013).
9. E. R. Brandao, C. H. Costa, M. S. Vasconcelos, D. H. A. L. Anselmo, and V. D. Mello, Opt. Mater. **46**, 378 (2015).
10. J. Da, Q. Mo, Y. Cheng, and T. Liu, J. Phys. **458**, 63 (2015).
11. D. Lusk, I. Abdulhalim, and F. Placido, Opt. Commun. **198**, 273 (2001).
12. J. Hendrickson, B. C. Richards, J. Sweet, G. Khitrova, A. N. Poddubny, E. L. Ivchenko, M. Wegener, and H. M. Gibbs, Opt. Express **16**, 15382 (2008).
13. V. Koju and W. M. Robertson, Opt. Lett. **41**, 2915 (2016).
14. K. Zhang, Y. Xu, T.-Y. Chen, H. Jing, W.-B. Shi, B. Xiong, R.-W. Peng, and M. Wang, Opt. Lett. **41**, 5740 (2016).
15. D. Zhang, Y. Zhang, W. Hu, Z. Li, and B. Cheng, Appl. Phys. Lett. **67**, 2431 (1995).
16. D. Zhang, W. Hu, Y. Zhang, Z. Li, B. Cheng, and G. Yang, Phys. Rev. B **50**, 9810 (1994).
17. H. Li, H. Chen, and X. Qiu, J. Phys. **279**, 164 (2000).
18. G. Alagappan and C. E. Png, Nanoscale **7**, 1333 (2015).
19. G. Alagappan and C. E. Png, Sci. Rep. **6**, 1 (2016).
20. T. W. Ren, J. L. He, C. Zhang, S. N. Zhu, Y. Y. Zhu, and Y. Hang, J. Phys. **16**, 3289 (2004).
21. A. A. Novikov and A. S. Chirkin, J. Exp. Theor. Phys. **106**, 415 (2008).
22. A. M. Vyunishev and A. S. Chirkin, Opt. Lett. **40**, 1314 (2015).
23. P. Yeh, A. Yariv, and C.-S. Hong, J. Opt. Soc. Am. **67**, 423 (1977).
24. Y. Zhang and Q. Wang, Optoelectron. Lett. **2**, 44 (2006).
25. A. Baldycheva, V. A. Tolmachev, T. S. Perova, Y. A. Zharova, E. V. Astrova, and K. Berwick, Opt. Lett. **36**, 1854 (2011).
26. S. E. Svyakhovskiy, A. I. Maydykovsky, and T. V. Murzina, J. Appl. Phys. **112**, 013106 (2012).
27. A. Yariv and P. Yeh, *Photonics: Optical Electronics in Modern Communications*, The Oxford Series in Electrical and Computer Engineering (Oxford University, 2007).